

## DYNAMIC ANALYSIS OF A MECHATRONIC DRIVE SYSTEM WITH AN INDUCTION MOTOR

YONGDI CAO, XIAOHONG LIU

*School of Mechanical Engineering, Yellow River Conservancy Technical Institute, Kaifeng, China*

*Corresponding author Yongdi Cao, e-mail: caoyongdi@yrcti.edu.cn*

The paper presents research findings in the modelling and optimization of dynamic parameters of mechatronic systems with an induction motor. A mathematical model was developed to analyze currents in dynamic states of squirrel-cage rotors in the case of a line-to-line fault. The findings were verified experimentally using calculations for a 1.5 kW three-phase induction motor. The equations for a stationary  $0x$ ,  $0y$  coordinate system relating to the stator were derived. The set of design variables selected in the optimization process contained parameters describing design features of the gear shafts and control units settings.

*Keywords:* dynamic model, electromechanical system, vector control, optimization, rotor

### 1. Introduction

In most cases, a mechatronic control object is a set consisting of an actuator (drive) and a certain technological or technical device, the operation of which is evaluated by the monitoring of process variables. A simple example would be combination of an electric motor and a machine (Draganescu *et al.*, 2003). An assembled servomotor – the kinematic unit – is a more complex control object. Status control here refers, for example, to the static position, or static position and velocity, and sometimes acceleration of moving units. This control is accomplished with object sensors that track the process. The information from the sensors is transmitted through a negative feedback loop to the control system. The mechatronic device operations result from the interaction of control, sensor and drive systems, as well as device programming by the operator.

Physical models of real-world objects are used for dynamic study of mechatronic objects. The outcome and reliability of computer simulation depends on appropriate simplifying assumptions. The model should take into account both the system main dynamic properties and main external forces applied to it. Proper selection of machine dynamic properties is one of the ways to improve the reliability and durability. Optimization techniques are increasingly being used to support this process. This is due to effectiveness of this approach as well as development of professional software and digital tools (Panchenko *et al.*, 2020). The initial application of optimization procedures dealt mostly with static problems, such as cost minimization, dimensions or maximization of the transmitted power, etc. (Gautam *et al.*, 2019). Sensitivity analysis and optimization are becoming a tool for solving complex problems of machine system dynamics and supporting the design process (Zhu *et al.*, 2019). Focus areas and development of structural optimization methods, starting from static problems and ending with the solution of dynamics problems, were discussed in Yang *et al.* (2021).

Optimization of dynamic systems requires development of physical models to mathematically describe the investigated phenomena (Syromyatnikov *et al.*, 2021). The frequency response determined on their basis is widely used in optimization, vibration level control and model improvement (Zhong and Ma, 2021). Intended functions are developed using the superposition principle as well as more complex hybrid methods (Korohodskyi *et al.*, 2021). Optimization studies are used to solve complex statical and dynamical problems in the fastest growing engineering industries, such as aviation (Panchuk *et al.*, 2020) and automotive ones (Kryshtopa *et al.*, 2019).

Typically, sensitivity analysis serves as an introduction to optimization studies. Its results are used to justify the choice of decision variables (Omelchenko *et al.*, 2019) and to evaluate the quantitative and qualitative influence of parameters on the intended functions that determine dynamic parameters of the systems. The easiest way to find the intended function derivatives is to use the finite difference method (German-Galkin and Kozak, 2018). This method has a very simple algorithm, but the results may be affected by numerical errors. The accuracy of this method is sufficient for solving moderately complex problems. Semi-analytical methods are much more accurate and faster, but require more work to prepare the data. These methods include direct and conjugate methods (Atiyah and Sulc, 2020). The derivatives of the intended function determine the areas of greatest growth of the function and can be used to optimize the design features of machine systems (Fediakov *et al.*, 2020). Symak *et al.* (2021) investigated the effectiveness of using the vector control in an induction motor to reduce dynamic loads in the kinematic pairs of an electric drive system (Gryzlov and Grigorev, 2019). Modeling the shape of a machine as a complex dynamical system consisting of a number of simple interacting subsystems is one method for determining the dynamic status of the machine. Mathematical models of machine drive systems are complex dynamic systems with many degrees of freedom (Rosenberg, 1966). Modeling an electric drive system as a system with feedback between its electrical and mechanical parts is an example of such an approach (Qiao *et al.*, 2018). Voltage sags, short-term power outages and phase shifts in the supply voltage are now considered among the most unpleasant electromagnetic interferences, including those attributed to the adverse effect on the receiver operation (Karlov *et al.*, 2021).

The equipment operation is primarily affected by the magnitude of the phase shift as well as the amplitude and duration of the voltage sag. Cirrincione *et al.* (2003) described simulation tests of an induction motor model with the resulting phase shift after voltage sag and restoration, as well as after the phase shift of the supply voltage occurring in steady-state mode.

A line-to-line fault also affects the supply side and should be considered for safety reasons. A line-to-line fault in an induction motor designed by Berhausen and Boboń (2018) usually occurs when the stator winding insulation is damaged by an electrical breakdown in the adjacent phase. A short circuit between phases (line-to-line fault) is random in its location, and it is impossible to determine where it will occur. Line-to-line faults depend, among other things, on:

- anomalies (switching-on, windings, stresses) occurring in the motor winding insulation;
- operating conditions (frequency of transient processes, operating temperature of the insulation), etc.

Line-to-line faults occur on the machine external terminals (Lohrasbi and Sahai, 1988). Available solutions differ in the way the velocity and torque are controlled and in the way the motor condition is evaluated (German-Galkin and Kozak, 2020). However, field monitoring is the most common method. When designing mechatronic systems, it is important to study dynamic parameters of the system, especially the electric drive, to ensure reliable and efficient operation of the designed system.

This study aims at analyzing the operation of asynchronous electric motors intended for use as parts of mechatronic systems. The objectives of the study are (1) to develop a dynamic mathematical model of an asynchronous electric motor; (2) to solve the resulting model in MATLAB/Simulink; (3) to investigate the dynamic performance parameters of the asynchronous motor under normal and two-phase short circuit conditions.

## 2. Methods and materials

This paper discusses a methodology for calculating the line-to-line fault with short circuit currents for a squirrel-cage rotor of the vehicle wheel drive. The design of mechatronic drive systems is among the main challenges facing the development of modern electric vehicles. In this study, the proposed model is applied to a mechatronic system. The system includes an asynchronous electric motor and a mechanical drive system. The wheel speed is controlled by a motor controller regulating the speed of an asynchronous electric motor attached to each wheel. The structure of the proposed mechatronic system is depicted in Fig. 1.

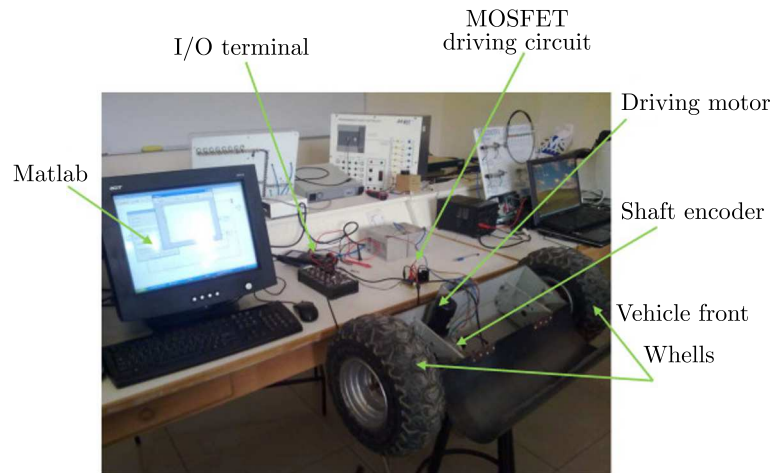


Fig. 1. Experimental mechatronic system

Mathematical modeling of the induction motor is based on the method of state variables. With this type of short-circuit, voltage spikes are important and are especially dangerous for the machine winding and the entire drive system (Rassõlkin *et al.*, 2020). The mathematical model of the motor has been developed in MATLAB to adopt dynamic parameters. The dynamic modeling of the line-to-line fault was based on the equations for state variables, chosen on the basis of the flux components:

- stator:  $\psi_{s\alpha}(t)$ ,  $\psi_{s\beta}(t)$ ,
- rotor output to the stator side:  $\psi_{rs\alpha}(t)$ ,  $\psi_{rs\beta}(t)$ ,
- velocity  $\omega$ .

At each time point, the iterated state variables were determined by the fourth order Runge-Kutta method for positive and negative symmetric components. The fourth order Runge-Kutta method has been widely used because of its simple implementation, relatively simple formulas, quick response and the method high order. It makes it possible to obtain satisfactory calculation results with a small iteration step.

The calculation of parameters and visualization were performed in Comsol Multiphysics. Table 1 shows the motor parameters.

**Table 1.** Induction motor parameters

Name	Expression	Value	Description
f0	60[Hz]	60 Hz	Supply frequency
w0	2*pi*f0	376.99 Hz	Supply angular frequency
n0	1000	1000	Number of turns
L	0.50[m]	0.50 m	Length of motor
Omega	160[rad/s]	160 rad/s	Rotor angular velocity
coil_wire_current	2045.175[A]*sqrt(2)/n0	2.8923 A	Current amplitude in coil wire
r1	2[cm]	0.020 m	Outer radius of rotor steel
r2	3[cm]	0.030 m	Outer radius of rotor aluminum
r3	3.2[cm]	0.032 m	Inner radius of windings
r4	5.2[cm]	0.052 m	Inner radius of stator steel
r5	5.7[cm]	0.057 m	Outer radius of stator steel
win_angle	45[deg]	0.7854 rad	Angular span of winding
airgap	r3-r2	0.0020 m	Size of air gap

### 3. Mathematical model of the induction motor in the case of a line-to-line fault

The equations of state adopted for an induction motor with a squirrel-cage rotor. The general form of differential equations for positive and negative components is given by

$$\begin{aligned}
\frac{d\psi_{sx}(t)}{dt} &= -x\psi_{sx}(t) + xK_r\psi_{rsx}(t) + u_{sx}(t) \\
\frac{d\psi_{sy}(t)}{dt} &= -x\psi_{sy}(t) + xK_r\psi_{rsy}(t) + u_{sy}(t) \\
\frac{d\psi_{rsx}(t)}{dt} &= -y\psi_{rsx}(t) + yK_s\psi_{sx}(t) - \omega(t)\psi_{rsy}(t) \\
\frac{d\psi_{rsy}(t)}{dt} &= -y\psi_{rsy}(t) + yK_s\psi_{sy}(t) + \omega(t)\psi_{rsx}(t) \\
\frac{d\omega}{dt} &= \frac{3p^2K_r}{2\sigma L_s J}\psi_{sy}(t) - \frac{3p^2K_r}{2\sigma L_s J}\psi_{sy}(t)\psi_{rsy}(t) - \frac{p}{J}M_z(t)
\end{aligned} \tag{3.1}$$

where:  $\sigma = 1 - (L_m^2/(L_s L_r))$  is the resulting dispersion coefficient;  $K_s = L_m/L_s$  – stator coupling coefficient;  $K_r = L_m/L_r$  – rotor coupling coefficient;  $x = R_s/(\sigma L_s)$ ,  $y = R_r/(\sigma L_r)$  – coefficients;  $u_{sx}(t) = U_s \cos(2\pi ft)$ ,  $u_{sy}(t) = U_s \sin(2\pi ft)$  – stator voltage along the  $x$  and  $y$  axis, respectively;  $R_s$ ,  $R_r$  – stator and rotor active resistance, respectively [Ohm];  $L_s$ ,  $L_r$ ,  $L_m$  – total stator, total rotor and magnetizing inductances [H].

The equivalent resistances and inductances for a serviceable asynchronous electric motor can be expressed as

$$R_e = R_s + R_r K_r^2 L_e = L_s - \frac{L_m^2}{L_r} \tag{3.2}$$

In the case of a line-to-line fault, a part of the phase stator winding will be short-circuited. In this case, the equivalent resistances and inductances for a serviceable asynchronous electric motor would be

$$R_e = R_s - R_{cs} + R_r K_r^2 \quad L_e = L_s - L_{cs} - \frac{L_m^2}{L_r} \tag{3.3}$$

where:  $R_{cs}$  is the faulty shorted part of the active resistance of the stator [Ohm];  $L_{cs}$  is the faulty shorted part of the stator inductance [H].

In these equations, five independent variables were chosen as the state variables:

- stator flux along the  $x$ -axis:  $\psi_{sx}(t)$ ;
- stator flux along the  $y$ -axis:  $\psi_{sy}(t)$ ;
- rotor flux recalculated to the stator side along the  $x$ -axis:  $\psi_{rsx}(t)$ ;
- rotor flux recalculated to the stator side along the  $y$ -axis:  $\psi_{rsy}(t)$ ;
- the angular velocity, electric  $\omega$ .

The excitation vector consists of the stator voltage along the  $x$ -axis and the stator voltage along the  $y$ -axis. The excitation vector consists of the moment loading the machine and the total moment of inertia which is assumed to be a constant for the purpose of line-to-line fault analysis. Hence, the excitation vector is a scalar (a given load torque). The angular velocity of the motor shaft  $\Omega$  expressed as the angular electric velocity  $\omega$  divided by the number of terminal pairs  $p$  is the output signal. The developed model takes into account both the possibility of setting the constant load torque and the load torque in the form of fan specifications depending on the machine rotational speed.

In the inductor motor model, the following simplifying assumptions are made:

- active resistances of the stator windings are identical;
- geometric axes of the sinusoidally distributed stator winding are separated by an angle of  $2\pi/(mp_n)$ , where  $p_n$  is the number of pole pairs;
- all phase  $m$  windings of the motor rotor (or  $m$  equivalent rotor windings) have identical active resistances  $R_r$  and identical quantities of pole pairs  $p_n$ ;
- geometric angle between the axes of rotor windings is equal to the angle between axes of stator windings;
- all parameters of the rotor are given to the stator winding;
- the machine has a symmetrical structure and the stator winding arrangement;
- isotropic sheet with no hysteresis loop was used in the calculations (Zhuravlev and Grigor'ev, 2018);
- calculations took into account the magnetic core saturation only in the areas of the teeth;
- shifting of currents in the winding conductors, affecting the values of resistance and inductance of stator and rotor windings, with each iteration depending on the operating state of this machine (Solodkiy *et al.*, 2018).

By defining the state variables as fluxes, the electromagnetic torque coming from the positive and negative components may be calculated

$$M_e = \frac{3pL_m}{2(L_sL_r - L_m^2)}[\psi_{sy}(t)\psi_{rsx}(t) - \psi_{sx}(t)\psi_{rsy}(t)] \quad (3.4)$$

After calculating the magnetic fluxes, the stator and rotor currents can be determined as in the substitute two-phase motor in the  $0x$  axis

$$i_{sx}(t) = \frac{\psi_{sx}(t) - K_r\psi_{rsx}(t)}{\sigma L_s} \quad i_{rsx}(t) = \frac{-K_r\psi_{sx}(t) + \frac{K_r}{K_s}\psi_{rsx}(t)}{\sigma L_s} \quad (3.5)$$

and  $0y$  axis

$$i_{sy}(t) = \frac{\psi_{sy}(t) - K_r\psi_{rsy}(t)}{\sigma L_s} \quad i_{rsy}(t) = \frac{-K_r\psi_{sy}(t) + \frac{K_r}{K_s}\psi_{rsy}(t)}{\sigma L_s} \quad (3.6)$$

The currents for individual motor phases are determined by the following expressions

$$i_{r1}(t) = i_x(t) \quad i_{r2}(t) = \frac{-i_{sx}(t)}{2} + \frac{\sqrt{3}}{2}i_{sy}(t) \quad i_{r3}(t) = \frac{-i_{sx}(t)}{2} - \frac{\sqrt{3}}{2}i_{sy}(t) \quad (3.7)$$

The model of an induction motor with an inter turn fault of the stator winding was built in MATLAB/Simulink using the SimPowerSystems block library for electrical systems (Fig. 2). In the model, stator winding A is shorted to represent the inter turn short circuit fault. To compare the currents, a serviceable motor model with similar parameters and no short circuit was added. In the experiment with asynchronous electric motors, 1:30 of the total turns on a phase winding turns were short-circuited in advance. When examining the inter turn short circuit of the stator winding, the hardware part involved a frequency converter with an open architecture based on a TMS320F28335 microcontroller (Texas Instruments). The frequency converter software relies on a built-in MexBIOS environment. The architecture of this environment enables control and diagnostic algorithms to be combined. A scalar control system was used to control the asynchronous motor, but the Mexbios Development Studio also permits the use of any algorithms for sensor and sensorless systems. The current of the faulty phase winding  $I_z$  is calculated from the measured values of the stator currents  $I_x$  and  $I_y$ .

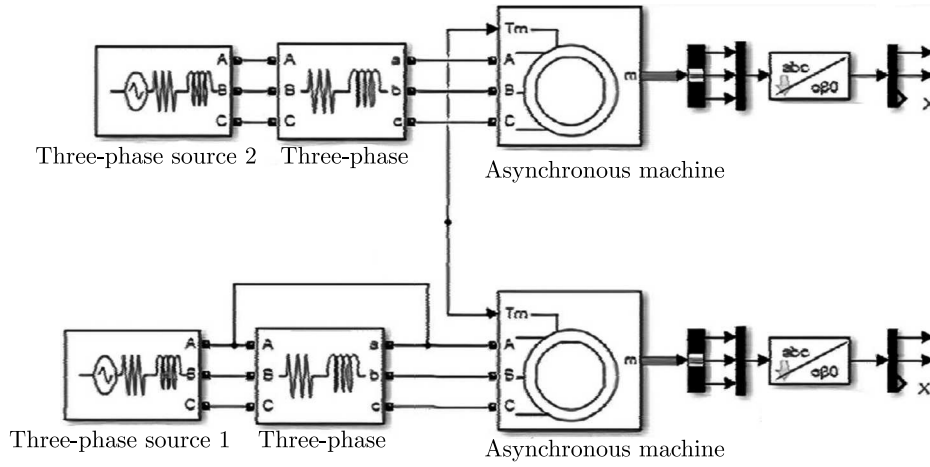


Fig. 2. Model of an asynchronous electric motor with an inter turn fault of the stator phase winding

#### 4. Results

To build a physical model of the analyzed drive system mechanical part, a hybrid method is used, which is a combination of the finite element method and the rigid finite element method. The gearing is modeled as a system of shafts resting on bearings, the masses of which are concentrated in the form of disks at the location of the gears. The shafts are connected to each other through mating gears. Bar elements are adopted to discretize the shaft. Non-deformable disks of the model gears are rigidly fixed in the assemblies for splitting the shaft into rod elements. The system is driven by an induction motor.

The numerical calculations relied on a monoharmonic induction motor model in the  $xy$  coordinate system. The motor equations with independent variables – stator current and rotor flux – are represented in the canonical form by five equations of state

$$\begin{aligned} \frac{di_{sx}}{dt} &= \frac{1}{L_z\sigma} \left\{ u_{sx} - R_s i_{sx} + \Omega_\phi \left( \sigma L_s i_{sy} + \frac{L_m}{L_r} \psi_{ry} \right) \right. \\ &\quad \left. - \frac{L_m}{L_r} \left[ u_{rx} - R_r \left( \frac{1}{L_r} \psi_{rx} - \frac{L_m}{L_r} i_{sx} \right) + (\Omega_\chi - p\Omega_m) \psi_{ry} \right] \right\} \\ \frac{di_{sy}}{dt} &= \frac{1}{L_z\sigma} \left\{ u_{sy} - R_s i_{sy} + \Omega_\chi \left( \sigma L_s i_{sx} + \frac{L_m}{L_r} \psi_{rx} \right) \right. \\ &\quad \left. - \frac{L_m}{L_r} \left[ u_{ry} - R_r \left( \frac{1}{L_r} \psi_{ry} - \frac{L_m}{L_r} i_{sy} \right) + (\Omega_\chi - p\Omega_m) \psi_{rx} \right] \right\} \end{aligned}$$

$$\frac{d\psi_{rx}}{dt} = u_{rx} - R_r \left( \frac{1}{L_r} \psi_{rx} - \frac{L_m}{L_r} i_{sx} \right) + (\Omega_\chi - p\Omega_m) \psi_{ry} \quad (4.1)$$

$$\frac{d\psi_{ry}}{dt} = u_{ry} - R_r \left( \frac{1}{L_r} \psi_{ry} - \frac{L_m}{L_r} i_{sy} \right) + (\Omega_\chi - p\Omega_m) \psi_{rx}$$

$$\frac{d\Omega_m}{dt} = \frac{1}{J} \left[ p \frac{L_m}{L_r} (\psi_{rx} i_{sx} - \psi_{ry} i_{sy}) - T_m \right]$$

$$T_e = pL_m (\psi_{rx} i_{sy} - \psi_{ry} i_{sx})$$

where:  $u_{sx}$ ,  $u_{sy}$  are components of the stator voltage vector (represented in the chosen Cartesian coordinate system);  $\Omega_m$  – rotor angular velocity;  $\Omega_\chi$  – angular velocity of the rotating biaxial system;  $\psi_{rx}$ ,  $\psi_{ry}$  – components of the rotor flux vector;  $i_{sx}$ ,  $i_{sy}$  – components of the stator current;  $T_e$  – electromagnetic torque.

The three-phase induction motor model has been visualized in Comsol Multiphysics. Figure 3 shows the resulting diagram.

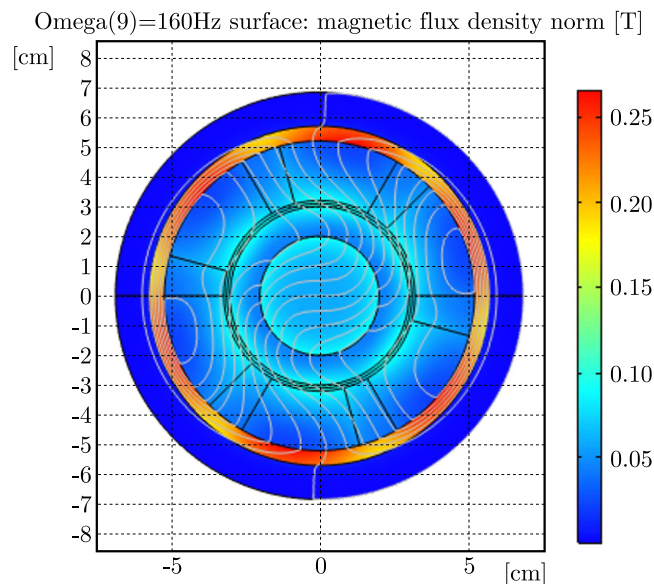


Fig. 3. Visualization of the magnetic field for the induction motor at  $\Omega_m = 160$  rad/s

To solve the mathematical model of the drive system as an electromechanical system, a software written in MATLAB/Simulink has been used. The preliminary calculations for the purpose of construction of the inertia, stiffness and damping matrix of the gear transmission and its connection with the housing were performed in MATLAB. A modal analysis of the analyzed mechanical of the drive system part was also performed in MATLAB. The model simulating dynamic problems of the electromechanical system was created in Simulink (Fig. 4).

This model incorporates vector control for the angular velocity with an inverter supplying the algorithm f. The shaft angular velocity is controlled by changing the frequency in the motor windings (Jia and Yan, 2019).

Table 2 compares the first 10 natural frequencies of the mechatronic system before and after using the reduction drive. The table clearly demonstrates that the approximation error of the first eight frequencies is less than 6%. In the case of natural frequencies before and after crimping, their complete relevance is validated for all the first 10 frequencies.

Table 3 shows the first ten natural frequencies of the drive system, the housing itself, and the model consisting of a gear wheel connected to the housing.

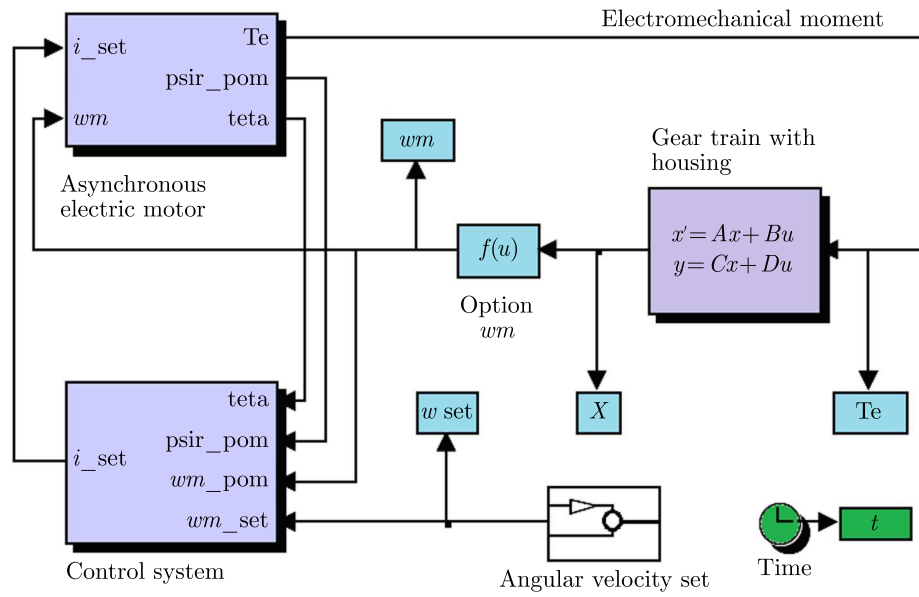


Fig. 4. Electromechanical model of a mechatronic system with an induction motor

**Table 2.** Comparison of natural frequencies of the housing model before and after reduction [Hz]

No.	Full model	Simplified model	Error [%]	$\chi^2$	SSD	$p$
1	367.57	375.86	1.15	0.99837	34.3621	< 0.005
2	410.03	430.35	1.45	0.99816	206.451	< 0.005
3	567.58	584.18	4.70	0.99656	137.780	< 0.005
4	583.88	611.48	4.78	0.99598	380.880	< 0.005
5	658.71	687.18	4.68	0.99379	405.270	< 0.005
6	667.43	688.53	4.65	0.99655	222.605	< 0.005
7	698.03	701.80	5.10	0.99916	7.10645	< 0.005
8	695.17	705.88	4.55	0.99970	57.3521	< 0.005
9	794.13	800.76	8.41	1.00000	21.9785	< 0.005
10	841.80	851.17	8.61	1.00000	43.8985	< 0.005

**Table 3.** Natural frequencies of the drive system [Hz]

No.	Drive system	Housing of reduction drive	Drive + housing
1	0	405.86	0
2	254.46	440.45	254.46
3	296.05	594.29	296.05
4	296.05	622.49	296.05
5	296.14	687.29	295.24
6	296.14	689.54	295.24
7	599.19	702.90	495.62
8	712.19	705.99	441.09
9	712.52	900.76	599.20
10	712.73	942.27	614.99

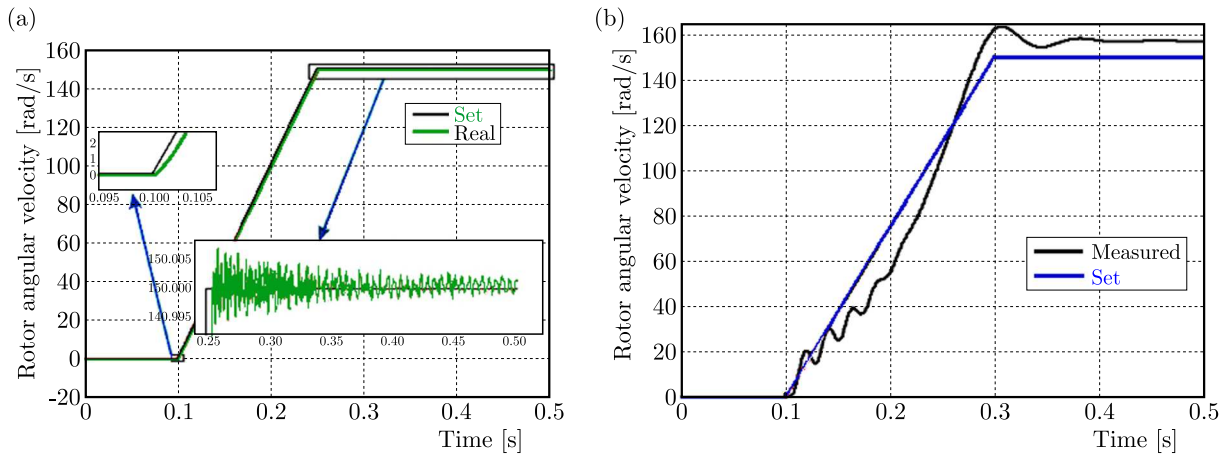


Fig. 5. Comparison of the set and actual rotational speed of the motor shaft

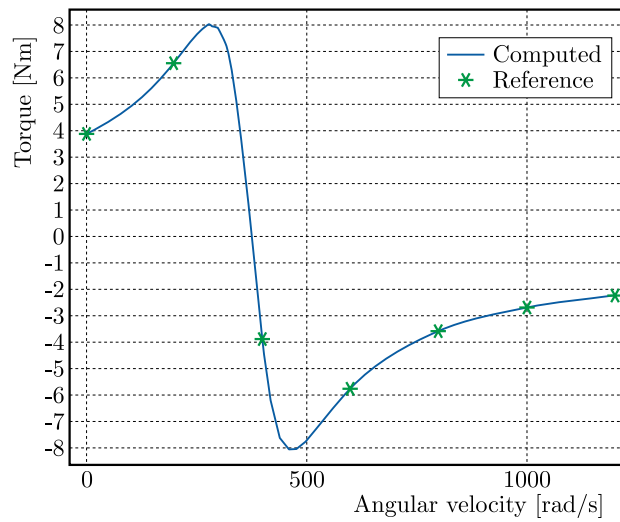


Fig. 6. Dependence of the torque on angular velocity

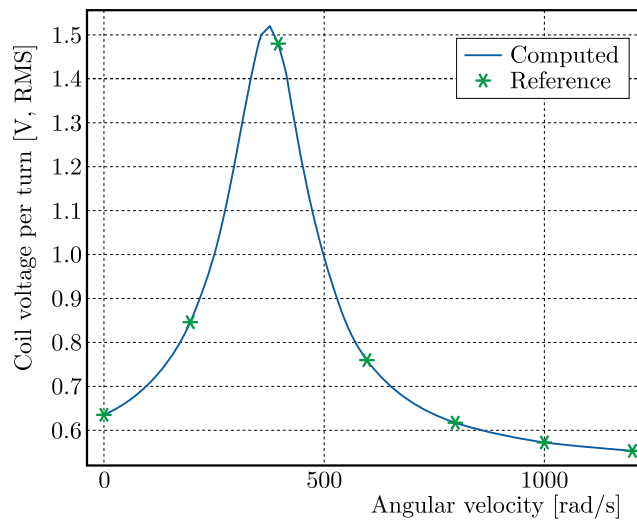


Fig. 7. Dependence of the coil voltage on angular velocity

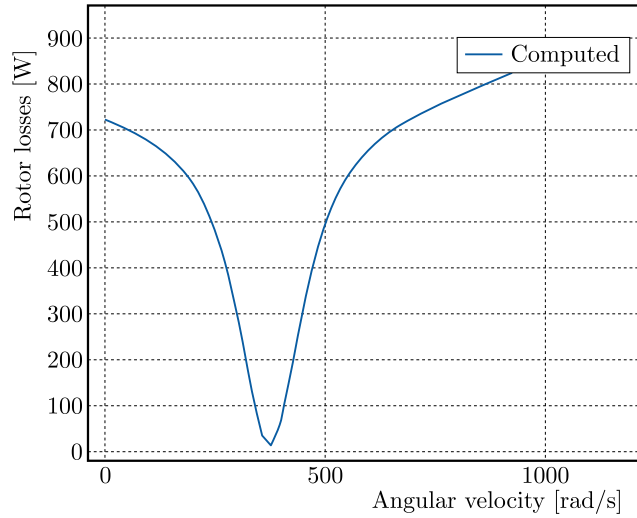


Fig. 8. Dependence of rotor losses on angular velocity

Figure 6 shows the calculated torque. Figure 7 shows the coil voltage, and Fig. 8 shows rotor losses as a function of rotational speed. The dependency graph shows the expected values for the induction motor. More specifically, the zero torque value, maximum voltage and minimum losses at the synchronous speed ( $\Omega = 370$  rad/s).

## 5. Discussion

The innovation of this study with respect to the vector control of a three-phase asynchronous motor is that the proposed motor model is relative simple and allows calculation of the modulus and phase of the rotor flux vector. These advantages eliminate the need for additional mathematical blocks that other models of three-phase asynchronous motors require. The frequencies along the axes ( $x, y$ ) are equal to zero, which enables higher accuracy and makes it easier to set up the circuits of three-phase asynchronous motors. The proposed model uses coordinate transformations that require knowledge of the position angle of the rotor flux vector calculated from the model. The coordinate transformation block operates with a delay of one sampling period, so this model requires a sufficiently high carrier frequency. In this case, the square root function is implemented through interpolation according to the table of reference points. It requires much more processor time and memory. Note that the presence of a block for calculating the amplitude and phase of the vector significantly complicates the implementation of the flux linkage meter.

Transient states occurring during dynamic operation of the induction motor depend on:

- machine power supply;
- changes in dynamic patterns of the applied external torque to the shaft (changes in the resulting moment of inertia of the entire system are possible) (Zhu *et al.*, 2019);
- mutual interaction of magnetic fluxes in transient states;
- form of voltage and current oscillations in specific phases of the stator and rotor windings, the currents associated with these windings.

With the discussed results of induction motor control in mind, the following properties of the drive system can be mentioned:

- the vector control enables full control of the motor torque and rotational speed;
- the rotational speed parameters are reproduced with high accuracy and small control deviations;

- control high quality is achieved with a constant value of the actual current component affecting the flux and with an adjustable imaginary component of the stator current which is proportional to the torque (Draganescu *et al.*, 2003).

The constant value of the rotor flux amplitude is achieved with a PI controller. The need to use coordinate transformation systems, which, unfortunately, affects the reliability and cost of such a system, constitutes the disadvantage of the chosen control method (Atiyah and Sulc, 2020). The resulting rotational speed and torque oscillograms reach a steady state after a short time without unnecessary oscillations. Starting the motor at the selected loads and the transition to the steady state takes a short time. The set speed is reached at idle speed in  $t < 0.3$  seconds. The control system significantly reduces motor inrush currents, which translates into a lower torque value in the initial phase of motor operation but increases the durability of its windings (Abbasi *et al.*, 2021). A lower starting torque value does not allow the rotor resistance to be overcome, so that the motor remains stationary during the initial starting phase. The shape of the phase currents obtained in the control system is close to sinusoidal and is subject to little distortion, which is a significant advantage of IFOC (Zhong and Ma, 2021). The control system response to a step change in the load is satisfactory, and the transition time to the steady state is a few ms (He *et al.*, 2020). The presented system makes it possible to control idling, which is not possible with scalar control methods. When calculating the transient states, first of all, a machine model should be developed with simplifying assumptions that allow for a mathematical description of the motor (German-Galkin and Kozak, 2018). The adopted equations of state for a squirrel-cage rotor were obtained for a stationary coordinate system associated with the stator. They describe electromagnetic wave forms in an equivalent three-phase induction motor (Symak *et al.*, 2021). Such a stationary coordinate system associated with the stator makes a relatively simple iterative simulation of a line-to-line fault possible. Because of this, the next iteration can be determined for each iteration from the previous moment by making vector composition of the positive and opposite components of the simulated machine (Solodkiy *et al.*, 2018). In the case of an induction motor, a different coordinate system rotating with constant or variable speed rigidly connected with the rotor causes a significant complication of equations and difficulty of analysis. This is because each iteration for both components must take into account the fact that the rotor speed at each iteration alternates with slip, which makes it difficult to compose vectors and calculate them (Rosenberg, 1966). Such a model provides equations relating the dependencies of the assumed state variables representing rotor rotation with respect to excitation in the form of voltages, currents, magnetic fluxes as well as load torque and solution inertia (Bast *et al.*, 2020). At each iteration, the system with the positive component and the system of equations with the inverse sequence have the same state, on the basis of which the state variables are calculated. Therefore, in each iteration, different values of the state variables are determined (for positive and negative components) based on the previous step and the conditions of feeding the specific symmetric component (German-Galkin and Kozak, 2018). The paper also provides a comparative analysis of the current flow in a low-power motor in this type of short-circuit. At this stage of model development, nonlinearities such as backlash and variable grid stiffness are excluded, and a monoharmonic induction motor model is adopted (He *et al.*, 2020). The direct torque control and the ability to influence the torque make it possible to achieve strong dynamic patterns with a fast response to changes in the set value of angular velocity.

## 6. Conclusions

The paper presents a dynamical model of a mechatronic system driven by an induction motor with a squirrel-cage rotor and vector control. The mechanical part takes into account the shaft and housing match. A system of differential equations describing electromagnetic wave forms

in an equivalent three-phase induction motor has been formulated, replacing spatial vectors with the corresponding relations between their components along the  $0x$  and  $0y$  axes for the direct sequence and a similar system of equations for the negative sequence. MATLAB and Comsol multiphysics were used to solve the model. Dependency graphs for parameters of the mechatronic drive system with the induction motor in operating conditions and with the squirrel-cage rotor in the vector control mode and without control were built. The research findings suggest that for a motor synchronous speed  $\Omega = 370$  rad/s the torque is zero, the voltage reaches its maximum value and the minimum rotor losses are observed. The diagnostic methods discussed earlier require either more calculations or preliminary settings for the induction motor. However, the comparative analysis of those methods provides qualitative results that are very useful in assessing suitability of the method. The main advantages of the proposed method are as follows: it is simple and demands less data processing. The proposed system is not limited to a laboratory bench and wheel drives of electric vehicles. The proposed electric drive design can be used in manufacturing industries and other mechatronic systems (cranes, air cooling systems, pumping units, etc.)

#### *Acknowledgments*

This research did not receive any specific grant from funding agencies in the public, commercial or non-profit sectors.

### References

1. ABBASI M.A., HUSAIN A.R., NIK IDRIS N.R., FASIH UR REHMAN S.M., 2021, Computationally efficient predictive torque control for induction motor drives based on flux positional errors and extended Kalman filter, *IET Electric Power Applications*, **15**, 6, 653-667
2. ATIYAH A., SULC B., 2020, Role of asynchronous motor modelling in driven railway wheelset dynamical simulation model, *2020 21th International Carpathian Control Conference (ICCC)*, 1-6
3. BAST D., KULCHYTSKA-RUCHKA I., SCHÖPS S., RAIN O., 2020, Accelerated steady-state torque computation for induction machines using parallel-in-time algorithms, *IEEE Transactions on Magnetics*, **56**, 2, 1-9
4. BERHAUSEN S., BOBOŃ A., 2018, Determination of high power synchronous generator subtransient reactances based on the waveforms for a steady state two-phase short-circuit, *Applied Mathematics and Computation*, **319**, 538-550
5. CIRRINCIONE M., PUCCI M., CIRRINCIONE G., CAPOLINO G.-A., 2003, A new experimental application of least-squares techniques for the estimation of the induction motor parameters, *IEEE Transactions on Industry Applications*, **39**, 5, 1247-1256
6. DRAGANESCU F., GHEORGHE M., DOICIN C.V., 2003, Models of machine tool efficiency and specific consumed energy, *Journal of Materials Processing Technology*, **141**, 1, 9-15
7. FEDIAKOV V.V., KORNIENKO M.N., ZHURAVLEVA L.A., 2020, Features of loss calculation in mechatronic modules on the basis of synchronous reluctance and induction AC electric drives, *2020 IEEE Conference of Russian Young Researchers in Electrical and Electronic Engineering (EIConRus)*, IEEE, St. Petersburg and Moscow, Russia, 639-643
8. GAUTAM P.V., KUSHWAHA H.L., KUMAR A., KUSHWAHA D.K., 2019, Mechatronics application in precision sowing: A review, *International Journal of Current Microbiology and Applied Sciences*, **8**, 4, 1793-1807
9. GERMAN-GALKIN S., KOZAK M., 2018, Structural model of the electric drive with double-fed asynchronous machine and direct torque control, *Multidisciplinary Aspects of Production Engineering*, **1**, 1, 41-45

10. GRYZLOV A.A., GRIGOREV M.A., 2019, Frequency-response methods for synthesizing controlled high-speed electric drives of compressors, *Russian Electrical Engineering*, **90**, 5, 364-369
11. HE S., SUI X., LIU Z., KANG M., ZHOU D., BLAABJERG F., 2020, Torque ripple minimization of a five-phase induction motor under open-phase faults using symmetrical components, *IEEE Access*, **8**, 114675-114691
12. JIA J., YAN X., 2019, Development and application of on-line torque telemetry system for rolling mill based on WIFI signal transmission and high frequency induction power supply, *Proceedings of the 3rd International Conference on Mechatronics Engineering and Information Technology*, 861-868
13. KARLOV D., PROKAZOV I., BAKSHTANIN A., MATVEEVA T., KONDRATENKO L., 2021, Optimizing neural network model performance for wind energy forecasting, *International Review on Modelling and Simulations*, **14**, 3, 185-193
14. KOROHODSKYI V., VORONKOV O., ROGOVYI A., KRYSHTOVA S., LYSYTSIA O., FESENKO K., BEZRIDNYI V., RUDENKO N., 2021, Influence of the stratified fuel-air charge pattern on economic and environmental indicators of a two-stroke engine with spark ignition, *AIP Conference Proceedings*, **2439**, 020011
15. KRYSHTOVA S., MELNYK V., DOLISHNII B., KOROHODSKYI V., PRUNKO I., KRYSHTOVA L., ZAKHARA I., VOITSEKHIVSKA T., 2019, Improvement of the model of forecasting heavy metals of exhaust gases of motor vehicles in the soil, *Eastern-European Journal of Enterprise Technologies*, **4**, 10 (100), 44-51
16. LOHRASBI J., SAHAI V., 1988, Magnetohydrodynamic heat transfer in two-phase flow between parallel plates, *Applied Scientific Research*, **45**, 1, 53-66
17. OMELCHENKO E., KHRAMSHIN T., TANICH V., KOZHEVNIKOV I., 2019, Dynamic computer model of traction asynchronous motor, *2019 IEEE Russian Workshop on Power Engineering and Automation of Metallurgy Industry: Research and Practice (PEAMI)*, 59-63
18. PANCHENKO A., VOLOSHINA A., TITOVA O., PANCHENKO I., CALDARE A., 2020, Design of hydraulic mechatronic systems with specified output characteristics, *Proceedings of the 3rd International Conference on Design, Simulation and Manufacturing: The Innovation Exchange*, Springer International Publishing, Cham, 42-51
19. PANCHUK M., KRYSHTOVA S., PANCHUK A., 2020, Innovative technologies for the creation of a new sustainable, environmentally neutral energy production in Ukraine, *International Conference on Decision Aid Sciences and Application, DASA 2020*, 9317165, 732-737
20. QIAO G., LIU G., SHI Z., WANG Y., MA S., LIM T.C., 2018, A review of electromechanical actuators for More/All Electric aircraft systems, *Proceedings of the Institution of Mechanical Engineers, Part C*, **232**, 22, 4128-4151
21. RASSÖLKIN A., BELAHČEN A., KALLASTE A., VAIMANN T., LUKICHEV D.V., ORLOVA S., HEIDARI H., ASAD B., PANDO ACEDO J., 2020, Life cycle analysis of electrical motor-drive system based on electrical machine type, *Proceedings of the Estonian Academy of Sciences*, **69**, 2, 162
22. ROSENBERG R.M., 1966, On nonlinear vibrations of systems with many degrees of freedom, *Advances in Applied Mechanics*, Elsevier, Amsterdam, **9**, 155-242
23. SOLODKIY E.M., DADENKOV D.A., KOSTYGOV A.M., 2018, Sensorless vector control of asynchronous machine based on reduced order Kalman filter, *2018 17th International Ural Conference on AC Electric Drives (ACED)*, *IEEE*, Piscataway, NJ, 1-5
24. SYMAK D., SABADASH V., GUMNITSKY J., HNATIV Z., 2021, Kinetic regularities and mathematical modelling of potassium chloride dissolution, *Chemistry and Chemical Technology*, **15**, 1, 148-152
25. SYROMYATNIKOV D., DRUZYANOVA V., BELOGLAZOV A., BAKSHTANIN A., MATVEEVA T., 2021, Evaluation of the economic profitability of using renewable energy sources in agro-industrial companies, *International Journal of Renewable Energy Development*, **10**, 4, 827-837

26. YANG J.Y., MING WANG D., GE Y.J., 2021, Design and implementation of hardware platform for bearingless induction motor control system, *2021 IEEE International Conference on Electrical Engineering and Mechatronics Technology (ICEEMT)*, Piscataway, NJ, 147-150
27. ZHONG B., MA L.L., 2021, Active disturbance rejection control and energy consumption of three-phase asynchronous motor based on dynamic system's decoupling, *Sustainable Energy Technologies and Assessments*, **47**, 101338
28. ZHU H., NESLER C., DIVEKAR N., AHMAD M.T., GREGG R.D., 2019, Design and validation of a partial-assist knee orthosis with compact, backdrivable actuation, *IEEE International Conference on Rehabilitation Robotics*, Piscataway, NJ, 917-924
29. ZHURAVLEV A.M., GRIGOR'EV M.A., 2018, Calculation of electric drives with electric machines of unconventional design, *Russian Electrical Engineering*, **89**, 4, 222-227

*Manuscript received August 4, 2022; accepted for print December 28, 2022*